

# Accurate determination of the sedimentation flux of concentrated suspensions

J. Martin, N. Rakotomalala, and D. Salin

Laboratoire Fluides Automatique et Systèmes Thermiques, Batiment 502, Campus Universitaire, 91405 Orsay Cedex, France

(Received 4 April 1995; accepted 31 May 1995)

Flow rate jumps are used to generate propagating concentration variations in a counterflow stabilized suspension (a liquid fluidized bed). An acoustic technique is used to measure accurately the resulting concentration profiles through the bed. Depending on the experimental conditions, we have observed self-sharpening, or/and self-spreading concentration fronts. Our data are analyzed in the framework of Kynch's theory, providing an accurate determination of the sedimentation flux  $[CU(C); U(C)$  is the hindered sedimentation velocity of the suspension] and its derivatives in the concentration range 30%–60%. In the vicinity of the packing concentration, controlling the flow rate has allowed us to increase the maximum packing up to 60%. © 1995 American Institute of Physics.

Sedimentation of noncolloidal suspensions has been formerly investigated by Kynch,<sup>1</sup> leading to the sedimentation velocity,  $U(C) = V_0 h(C)$ , where  $V_0$  is the Stokes settling velocity of a single particle,  $C$ , the volume fraction, and  $h(C)$ , the concentration-dependent settling function, accounting for hindrance due to backflow phenomena.<sup>2</sup> While the low concentration regime is readily resolved, with reasonable agreement between theory<sup>2</sup> and experiments,<sup>3</sup> the high concentration regime is still a theoretical challenge.<sup>4</sup> Experimental investigations at larger concentrations are more or less in reasonable agreement with the empirical relation of Richardson–Zaki,<sup>5</sup>  $h(C) = (1 - C)^p$ , where  $p$  is an adjustable parameter that depends on the Reynolds number ( $p \sim 5.5$  at low  $Re$ ), and most likely on the residual polydispersity of the nearly monodisperse suspension. Such a routinely used relation is usually acceptable in most applications, even if it does not perfectly match the low concentration prediction. Indeed, the lack of accuracy of this determination appears when addressing the two issues of front propagation in suspensions<sup>6–8</sup> and fluidized bed stability,<sup>9,10</sup> which require a precise determination of not only the sedimentation flux,  $F(C) = CU(C)$ , but also of its derivatives. A rapid inspection of  $F(C)$  shows that flux variations in the range 40%–60% are very close to a straight line. Therefore, accurate measurements are needed in order to determine curvature and inflection. In order to avoid the sedimentation problem inherent to achieving a homogeneous suspension, we use, once again,<sup>7–12</sup> a liquid fluidized bed as a counterflow stabilized suspension, which provides a reproducible stirred suspension stationary in the laboratory frame of reference (note that there is some size segregation that leads to a small and therefore negligible concentration gradient along the bed). Monitoring the counterflow allows to control the relative sedimentation of the suspension and to propagate concentration jumps throughout the bed. Using an acoustic technique<sup>14</sup> to measure the shape of the concentration profile (i.e., concentration variations) inside the bed, we determine, from Kynch's approach, the sedimentation normalized flux  $f(C) = Ch(C)$  and its derivatives for concentrations up to the packing one.

For a homogeneous suspension of monodisperse spherical particles of radius  $a$  at a concentration  $C$ , the sedimentation process is governed by the conservation of particles,

$$\partial C / \partial t + \partial J / \partial x = 0, \quad (1)$$

where  $J = CV_p$  is the particle flux and  $C(x, t)$  is the volume fraction. Here  $V_p$  is the particle velocity (all velocities are algebraic quantities, the vertical direction  $x$  is oriented downward). In the absence of concentration gradients,<sup>7,13</sup>

$$V_p - V = U(C), \quad (2)$$

where  $V = CV_p + (1 - C)V_f$  is the mean velocity of the suspension and  $V_f$  is that of the fluid. For a fluidized bed at a counterflow rate per unit area,  $q$ ,  $V = -q$  in the laboratory frame of reference. Still omitting hydrodynamic dispersion effects, the response of the bed to a flow rate decrease from an initial value  $q_0$  to  $q$  follows from Eq. (1):

$$\partial x / \partial t|_c = dF(C) / dC - q, \quad (3)$$

which gives the traveling velocity of the concentration  $C$ .<sup>1</sup> Depending on the shape of the sedimentation flux curve,  $F(C) = CU(C)$ , and on the flow rate jumps, this equation leads to self-spreading (the traveling velocity increases with the concentration without conflict) or self-sharpening (certain concentrations overtake the other, leading to a shock) of the concentration fronts, or to a combination of the two processes. Typical sketches, relevant to the bed experimental device, are given in Fig. 1. On each  $F(C)$  graph, the full straight line corresponds to the initial flux  $q_0 C$ ,  $q_0 = U(C_0)$ , and the dashed one to the final flux  $q C$ . In Fig. 1(a), Kynch's construction [dashed bold chord, above  $F(C)$ ] leads to a self-spreading front, in which case, from Eq. (3), one gets the flux derivative between  $C_0$  and  $C_m$ . This sketch depicts the fluidized bed situation for a flow rate jump from  $q_0$  down to the minimum fluidization flow rate  $q_m$ . Figure 1(b) relates to the suspension sedimentation case: the equivalent final flow rate,  $q$ , is zero, and the dashed bold chord lies almost below the flux curve, leading to a shock front at the bottom of the suspension. This unfortunately prevented us from a direct determination of the flux.<sup>15</sup> Note that a fluidized bed allows

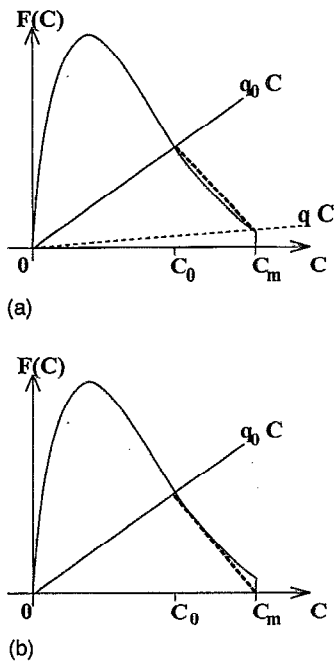


FIG. 1. Schematic of the fluidized bed (a) and settling suspension (b) experimental situations. Here  $F(C)$  is the sedimentation flux function. The full  $q_0 C$  and dashed  $q C$  straight lines correspond to the initial  $q_0$  and the final  $q$  flow rates ( $q=0$ , for settling). The dashed bold chord is Kynch's construction. In (a), the chord is above the flux curve, leading to a self-spreading concentration profile. In (b), the chord lies below, leading to a shock front at the bottom of the settling suspension.

for scanning of the flow rate region between  $q_m$  and 0, leading to the possible occurrence of a mixed situation, where both self-spreading and a shock front are encountered [a dashed bold chord crossing  $F(C)$  at  $C_c$  leads to a shock front between  $C_m$  and a concentration given by the tangent construction.<sup>1</sup> The design of the experiment is straightforward: the best choice corresponds to Fig. 1(a) with the widest concentration range, i.e., between  $C_m$  and the inflection point of  $F(C)$ .

Experiments were performed in a column 60 cm high of a circular cross section (4 cm). We determine the concentration profile by measuring variations in the sound speed in several cross sections along the bed.<sup>11</sup> We estimate the overall accuracy in concentration measurements to be 0.1% and the spatial resolution to 1 mm. The liquid used is a water-glycerol mixture ( $\eta=2.10^{-3}$  Pa s). The spherical glass beads have a diameter  $2a=68.5 \mu\text{m}$ , with 95% of the particles in the range 63–74  $\mu\text{m}$ . In the experiments, the particle Reynolds number ( $Re = U_0 a \rho_f / \eta$ ) is less than 0.1. To take advantage of the method, we choose a large concentration jump between  $\sim 30\%$  and the packing concentration  $\sim 57\%$ ,<sup>15</sup> but with different final flow rates down to zero in order to investigate in detail the vicinity of the packing (i.e., the minimum fluidization velocity<sup>9</sup>). This is a definite breakthrough of the fluidized bed compared to a sedimentating suspension for which  $V$  (or  $q$ ) is always zero. Figures 2 and 3 show concentration profiles at different locations along the column for a flow rate jump from  $q_0=0.0345$  cm/s,  $C_0 \sim 30\%$  to  $q=0.0023$  cm/s, and from  $q_0=0.0383$  cm/s to  $q=0.0015$  cm/s, respectively. In Fig. 2, the front profile is spreading for

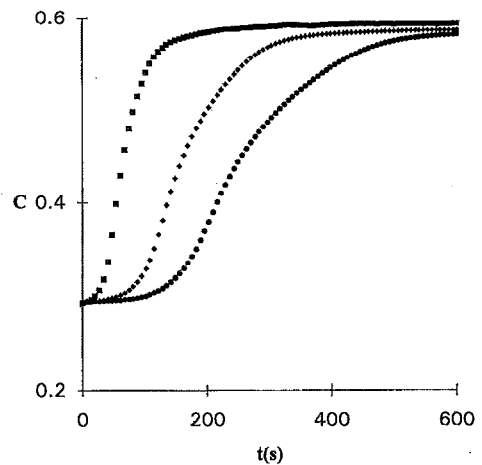


FIG. 2. Self-spreading profiles. Concentration versus time at three different vertical positions ( $x=2, 5$ , and  $8$  cm from the bottom inlet) for a flow rate jump from  $q_0=0.0345$  cm/s to  $q=0.0023$  cm/s.

any concentration, whereas in Fig. 3, the front exhibits both a spreading part at low concentration and a shock front at larger concentration. The first experiment illustrates Fig. 1(a), whereas the second one corresponds to a case in between Figs. 1(a) and 1(b). From the three profiles (at three “long time” locations, which allows for neglecting hydrodynamic dispersion) of Fig. 2, we can determine the velocity of each concentration ( $\partial x / \partial t|_C$ ), which gives the first derivative of the sedimentation flux. In order to get results suitable for comparison, we normalize the sedimentation flux by the Stokes velocity:  $f(C) = F(C) / V_0 = Ch(C)$ . Here  $V_0$  is computed with the mean particle size; its value is found to agree with the zero-concentration value extrapolated from our sedimentation velocity data. In Fig. 4, we plot  $f'(C) = df(C) / dC$  vs  $C$  from our data of Figs. 2 and 3. For the latter dataset, the shock front is responsible for the plateau at large concentration: for all concentrations involved in this shock, the traveling velocity is the same and is given by the slope of the corresponding chord [Fig. 1(b)]. In Figs. 2–3, the slopes near maximum and minimum concentration

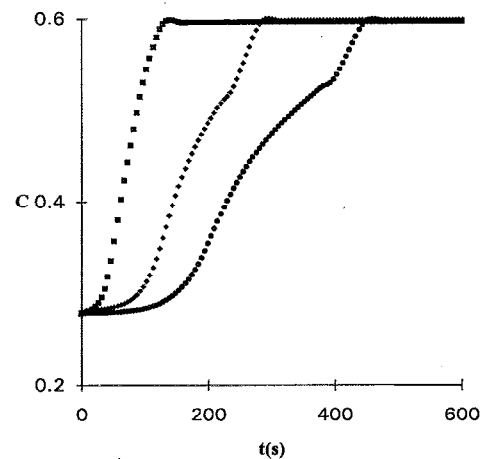


FIG. 3. Spreading and shock fronts. The same as Fig. 2, but for a jump from  $q_0=0.0383$  cm/s to  $q=0.0015$  cm/s.

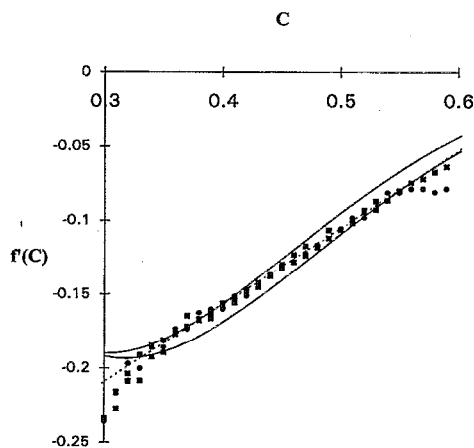


FIG. 4. Derivative,  $f'(C) = df(C)/dC$ , of the normalized sedimentation flux function  $f(C)$ . Full squares correspond to the concentration profiles of Fig. 2, full circles to Fig. 3. The full lines are the Richardson-Zaki relation with exponents  $p=5.6$  (top) and  $p=5.3$  (bottom). The dashed line is a linear best fit to the data.

are difficult to determine, reducing the accuracy for these data. The two solid lines correspond to the Richardson-Zaki relation<sup>5</sup> with the exponents  $p=5.6$  and  $p=5.3$  for the top and bottom curves, respectively. Even though such a relation is in good agreement with our data, we note that in this concentration range (30%–60%) the first derivative of the flux is mainly linear in  $C$  (dashed straight line of Fig. 4), and hence the second derivative is constant (positive: upward curvature). In Fig. 5, we plot the normalized sedimentation flux,  $f(C)$ , versus the concentration. Squares correspond to data for which  $h(C)$  was determined from the bed expansion (its height); the nearly uniform concentration is controlled by acoustics. The full curve is the best fit with the Richardson-Zaki relation<sup>5</sup> (exponent  $p=5.35$ ; this fit leads to  $V_0$ ), while the dashed line is obtained through integration of our flux derivative curve (Fig. 4). Above 30% concentration, the data and the two fits are in reasonable agreement. We emphasize

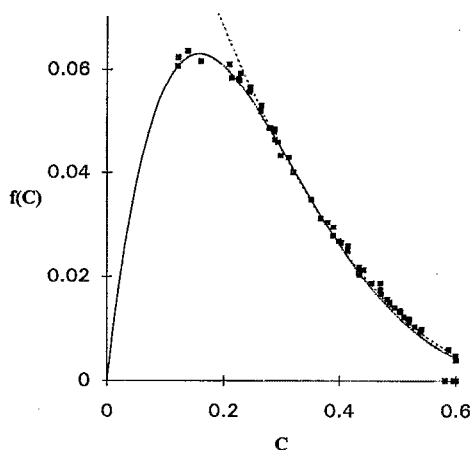


FIG. 5. Normalized sedimentation flux  $f(C) = Ch(C)$  versus concentration  $C$ . The full squares are measured from the bed expansion. The full curve is the Richardson-Zaki best fit to our data ( $p=5.35$ ). The dashed straight line is obtained from an integration of Fig. 4.

that even though Richardson-Zaki relation is obtained from a data fit to  $U(C)$ , this relation is robust when compared to the data of the flux function and its derivatives. One can observe that, in our dataset, we do get concentrations up to nearly 60%. Indeed, these high values of packing concentrations are obtained in the following experimental conditions. For large initial flow rates corresponding to low initial concentration, switching off the flow rate, leads to a classical (well-stirred) sedimentation, and we get a packing concentration of  $C_m \sim 57\%$ , in agreement with previous experiments.<sup>15</sup> Starting with large concentrations (above 50%) enhances the packing concentration slightly. The largest packing concentrations are achieved when tuning the flow rate down to the minimum fluidization value; these high values remain when switching the flow rate. Such a systematic effect has not been previously noticed in settling suspension, when increasing the initial concentration. The closer the initial concentration is to the packing one, the larger the final packing value: the suspension, as we reduce the flow rate, is able to pack itself in a denser arrangement.

Analyzing the time and space concentration response of a stable fluidized bed to flow rate jumps allows for an accurate determination of the derivative of the suspension flux function at large concentration, and especially in the vicinity of the packing concentration. Our results are consistent with the Richardson-Zaki relation, with  $p=5.35$  at a low Reynolds number, but also with an almost linear fit for  $df(C)/dC$ , leading to a nearly constant upward curvature of the flux between 40% and 60%. In the procedure of approaching the minimum fluidization flow rate, we have observed a net increase of the packing concentration up to 60%.

<sup>1</sup>G. J. Kynch, "Theory of sedimentation," *Trans. Faraday Soc.* **48**, 166 (1952).

<sup>2</sup>G. K. Batchelor, "Sedimentation in a dilute dispersion of spheres," *J. Fluid Mech.* **52**, 245 (1972).

<sup>3</sup>R. H. Davis and K. H. Birdsell, "Hindered settling of semidilute monodisperse and polydisperse suspensions," *AIChE J.* **34**, 123 (1988).

<sup>4</sup>A. J. C. Ladd, "Dynamical simulations of sedimenting spheres," *Phys. Fluids A* **5**, 299 (1993), and references therein.

<sup>5</sup>J. F. Richardson and W. N. Zaki, "Sedimentation and fluidization: Part 1," *Trans. Inst. Chem. Eng.* **32**, 35 (1954).

<sup>6</sup>J. Martin, N. Rakotomalala, and D. Salin, "Hydrodynamic dispersion broadening of a sedimentation front," *Phys. Fluids Lett.* **6**, 3215 (1994).

<sup>7</sup>J. Martin, N. Rakotomalala, and D. Salin, "Hydrodynamic dispersion of noncolloidal suspensions: Measurement from Einstein's argument," *Phys. Rev. Lett.* **74**, 1347 (1995).

<sup>8</sup>G. B. Whitham, *Linear and Non-linear Waves* (Wiley, New York, 1974).

<sup>9</sup>T. B. Anderson and R. Jackson, "Fluid mechanical description of fluidized beds," *Ind. Eng. Chem. Fundam.* **7**, 12 (1968).

<sup>10</sup>G. K. Batchelor, "A new theory of the instability of a uniform fluidized bed," *J. Fluid Mech.* **193**, 75 (1988).

<sup>11</sup>*Fluidization*, edited by J. F. Davidson, R. Cliff, and D. Harrison (Academic, London, 1985).

<sup>12</sup>J. Z. Xue, E. Herbolzheimer, M. A. Rutgers, W. B. Russel, and P. M. Chaikin, "Diffusion, dispersion in settling of hard spheres," *Phys. Rev. Lett.* **69**, 1715 (1992), and references therein.

<sup>13</sup>R. H. Davis and M. A. Hassen, "Spreading of the interface at the top of a slightly polydisperse sedimenting suspension," *J. Fluid Mech.* **196**, 107 (1988).

<sup>14</sup>J.-C. Bacri, M. Hoyos, N. Rakotomalala, D. Salin, M. Bourlion, G. Daccord, R. Lenormand, and A. Soucemarianadin, "Ultrasonic diagnostic in porous media and suspensions," *J. Phys. France III* **1**, 1455 (1991).

<sup>15</sup>J.-C. Bacri, C. Frenois, M. Hoyos, R. Perzynski, N. Rakotomalala, and D. Salin, "Acoustic study of suspension sedimentation," *Europhys. Lett.* **2**, 123 (1986).